

BEHAVIOR OF CONCRETE BEAMS REINFORCED IN SHEAR WITH CARBON FIBER REINFORCED POLYMER

Dr. Abdul-Muttalib I. Said Al-Mussaue
Ass. Prof
University of Baghdad
College of Engineering

Mr. Amjad H. Abdul-Razaq Al-Modhafer
Ass. Lecturer
University of Kufa
College of Engineering

ABSTRACT

Carbon fiber reinforced polymers (CFRP) were widely used in strengthening reinforced concrete members in the last few years, these fibers consist mainly of high strength fibers which increase the member capacity in addition to changing the mode of failure of the reinforced concrete beams. Experimental and theoretical investigations were carried to find the behavior of reinforced concrete beams strengthened by CFRP in shear and bending. The experimental work included testing of 12 beams divided into 4 groups; each group contains 3 beams. The following parameters were taken into consideration:

- Concrete crushing strength.
- CFRP strengthening location (shear strengthening and both shear and flexure strengthening).

Reinforced beams were simply supported subjected to two point loads. Each group consists of three beams; the first beam without CFRP, the second one, is strengthened with CFRP in shear and the third is strengthened with CFRP in both flexure and shear. Four groups with different crushing strength of (12, 20, 30 and 39 MPa). The CFRP sheets are attached externally.

It was found that in beam with low crushing strength loads transfer to the CFRP at early stages while in those of high crushing strength, CFRP contribution only starts when full strength of the beam is fulfilled. A full bond between CFRP sheets and the concrete is assumed in the theoretical analysis. Comparison between the theoretical and the experimental results revealed the validity of the numerical analysis and the developed methods such that there was a difference of 13% in the ultimate strength for the tested and analyzed beams.

خلاصة:

استعملت العناصر الإنشائية الخرسانية المسلحة المقواة بألياف البوليمر الكربونية في السنوات الحديثة ، تتألف ألياف التقوية البوليمرية بصورة أساسية من ألياف (عالية المقاومة) حيث تزيد سعة التحمل بالإضافة إلى تغيير أسلوب الفشل للعتبات الخرسانية المسلحة. أجريت تحريات عملية ونظرية لسلك العتبات الخرسانية المسلحة، لحالتي تقوية العتبات في مناطق فشل القص والانشاء المقواة باستخدام CFRP حيث يتكون البرنامج العملي من 12 عتبة فحص قسمت إلى أربعة مجاميع ، كل مجموعة تضم 3 عتبات. الدراسة أخذت بنظر الاعتبار مقاومة الانضغاط للخرسانة و حالة التقوية ، استعملت مرة للتقوية في منطقة القص وأخرى في منطقتي القص و الانشاء معاً بكل العتبات تم فحصها في فضاء بسيط الإسناد ومتعرض لنقطتي تحميل بينما المتغير الرئيس يمثل مقاومة الانضغاط للخرسانة و موقع CFRP. كل مجموعة تتكون من ثلاثة عتبات الأول وهو النموذج المرجعي وهو خالي من CFRP و الثاني يحتوي على CFRP في منطقة القص و هي عبارة عن سبعة شرائح مائلة بزاوية 45 درجة و الثالث يحتوي على CFRP في منطقتي القص و الانشاء.

كل مجموعة لها مقاومة انضغاط مختلفة عن الأخرى وهي (12-20-30-39 MPa). استعمل CFRP كمقوي خارجي. أن استعمال CFRP له تأثير على نتائج الحمل الأقصى، شكل التشقق، الهطول. تم اكتشاف أن CFRP يشارك الخرسانة الضعيفة في أوقات مبكرة من الحمل بعكس الخرسانة التي لها قوة انضغاط عالية حيث تتحمل أولاً هي لوحدها جميع الاجتهادات ثم تشاركها شرائح CFRP في التحمل. إن أفضل استخدام لشرائح CFRP في منطقة القص بسبب تحول القوى بصورة مباشرة إلى شد على هذه الشرائح.

تم استعمال التحليل اللاخطي بواسطة العناصر ثلاثية الأبعاد لتحري أداء العتبات الخرسانية المسلحة المقواة ب CFRP ، حيث تم استخدام البرنامج الحاسوبي ANSYS.

اعتبرنا هنالك تماس تام بين شرائح CFRP والخرسانة. وتم الحصول على تنبؤ جيد لسلوك ما بعد التصدع. المقارنة بين النتائج النظرية والعملية أكدت صلاحية التحليل العددي و حيث كانت أكبر نسبة فرق في المقاومة القصوى أقل من 13 % لكل العتبات المفحوصة.

Keywords: Crushing strength, CFRP, Shear, Inclined strips, flexure, strengthening

INTRODUCTION:

A carbon fiber sheet is formed by laying out fibers in single or multiple directions and embedding in a protective epoxy resin. A carbon fiber sheet receives particular attention due to its higher strength, stiffness, corrosion and fatigue resistance with reasonable cost. One advantage of using a fiber composite material is the negligible increase in dead load due to its light weight; in addition, it can be easily carried to construction site in rolls. Because the reinforcing technique is much simpler with fiber composite, strengthening/retrofitting work is more convenient in a limited workspace and no specific work experience and heavy construction equipment are required at the site.

Carbon fiber sheet has a very high unidirectional tensile strength but has stiffness close to that of steel. Typical values are between 2500-4600 MPa for tensile strength and 235-269 GPa for Young's modulus. The behavior is essentially linearly elastic up to the tensile strength limit. Once it reaches its tensile strength, it fails in a perfectly brittle model, **Figure 1**. Fibers are assumed to have strength and stiffness only in the fiber direction and no resistance perpendicular to the fiber direction is considered. Because of its negligible thickness, carbon fiber sheet exhibit no effective compression or bending stiffness. Taking the above characteristics into account, a finite element with only axial stiffness is used to represent carbon fiber in structural analysis.

Fiber materials commonly used are carbon, glass or aramid. The different FRP materials and systems have varying properties and behavior. A qualitative comparison of the performance of carbon, glass, and aramid composites is presented in **Table 1**.

This carbon fiber used to manufacture an unidirectional tow sheet that has a width off 330 mm and is suitable for applications requiring a wet lay-up process to conform to the surface configuration of the structure as shown in **Figure 2**.

EXPERIMENTAL WORK:

The experimental program consisted of testing twelve simply supported beams. Beams with rectangular cross sections of 150 mm width by 280 mm height and 3350 mm length. A span between supports of 3200 mm and distance between loads of 1200 mm. The longitudinal reinforcement consists of three No.16 bars (16-mm-dia.) in tension and two No. 10 bars (10-mm-dia.) in compression, equivalent to reinforcement ratios of $\rho=0.0157$ and $\rho'=0.0041$, respectively.

Figures 3 and 4 show specimen dimensions, reinforcement details, support locations, and location of loading points.

No shear reinforcement in tested beam to ensure that shear failure in happen before bending failure.

In order to identify the test specimens with different strengthening schemes and different concrete strengths, the following designation system is used as list in **Table 2**:

Figures (4), show the reinforced concrete beams with CFRP in shear and flexure zone (side and bottom view).

TESTING PROCEDURE:

All beams were tested in a universal testing machine, with maximum capacity of 2000 kN. Beam was loaded directly at the top face with two equal concentrated loads. The ends of all beams were extended 125mm beyond the supports centerline to provide adequate anchorage for the longitudinal steel. 60mm x150mm bearing plates were used at loading points and at supports to avoid local crushing of concrete. The beams were tested under static loads, loaded in successive increments up to failure. For each increment, the load was kept constant until the required readings were recorded.

Demec points were used for each tested beam at mid-span on concrete surface and CFRP shown in **Figures 5** and the initial distance between each two horizontal Demec points were calibrated using an accompanying special ruler.

TEST RESULTS

The ultimate load and mid span deflections at cracking and ultimate stages are shown in **Table 4**. The same mode failure occurred for all beams. This mode was a diagonal shear crack causes rupture of all CFRP sheets located in the shear zone at ultimate load level. Discussion of results obtained for each group is presented in the following sections. The beams before tested are shown in **Figures 6**.

CRACK PATTERNS AND FAILURE MODE:

The loads are applied gradually up to failure. **Figure 7** shows crack patterns of all tested beams.

The sketch the map of cracks of *BC1*, *BC2*, *BC3* and *BC4* shown in **Figures 8**.

LOAD AGAINST MID-SPAN DEFLECTION:

From the load deflection curves of the tested beams it can be observed that the load against mid-span deflection response can be divided into three stages of behavior. In the first stage, a linear behavior of the load deflection response is observed. In the second stage, a nonlinear behavior of the load deflection response is noticed. Finally in third stage, as the applied load reaches near its ultimate value, the rate of increase in deflection is substantially exceeding the rate of increase in the value of the applied loads. **Figure 9**, shows the load-deflection for beams having same crushing strength at $f'_c=12, 20, 30$ and 39 MPa respectively.

FINITE ELEMENT MODEL:

The tested beams where analyzed using **ANSYS** program (**ANSYS** 2005 version 10). Four different materials are involved concrete, reinforcement, steel plates, and CFRP strips.

Concrete: the solid 65, 3-D reinforced concrete solid element was used to represent concrete in the models. The element using a $2 \times 2 \times 2$ Gaussian set of integration points is defined by eight nodes having three degrees of freedom at each node: translations in the nodal x, y, and z directions. This element is capable of cracking in tension and crushing in compression.

Steel: the solid 45 is used for the 3-D modeling of structural members steel bearing plates located at supports and under the applied loads.

Reinforcement: The link 8 element is a uniaxial tension-compression element with three degrees of freedom at each node, translations in the nodal x, y, and z directions. This element is used to represent the steel bars.

CFRP Sheets: Solid 46 is a layered version of the 8-node structural solid designed to model layered thick shells or solids. The element allows up to 250 different material layers. In present study, this element is used to represent CFRP strips.

Tested beams are $150 \text{ mm} \times 280 \text{ mm} \times 3350 \text{ mm}$; with a span between supports of 3200 mm . **Figure 10**, illustrates typical dimensions for all four beams before CFRP reinforcing. By taking advantage of the symmetry of the beams, a quarter of the full beam was used for modeling. This approach reduced computational time and computer disk space requirements significantly. A quarter of the beam model is shown in **Figure 11**.

Figure 12 shows typical steel reinforcement for a quarter beam model.

Ideally, the bond strength between the concrete and steel reinforcement should be considered. However, in this study, perfect bond between materials was assumed. To provide the perfect bond, the link element for the steel reinforcing was connected between nodes of each adjacent concrete solid element, so the two materials shared the same nodes. The same approach was adopted for CFRP composites. The high strength of the epoxy used to attach CFRP sheets to the beams supported the perfect bond assumption.

ANALYTICAL RESULTS:

The accuracy of the finite element modeling is determined by ensuring that the ultimate load is reasonably predicted in comparison with the experimental results, and the load-deflection curves are close to the experimental curves as well as the crack patterns are similar to that obtained from experimental test.

Comparison of the load-deflection curves, cracking loads, ultimate load carrying capacity and crack pattern by the finite element analysis and the laboratory tests is made.

The ratios of the predicted finite element ultimate loads to the corresponding experimental ultimate loads of the analyzed beams are listed in **Table 5**.

NUMERICAL LOAD VERSUS MID-SPAN DEFLECTION:

Figures 13 shows the load versus mid-span deflection curves for the finite element analyses and experimental results for beams.

Several conclusions are drawn from may be notice from comparison between experimental and analytical case studies.

- The theoretical results are nearby the experimental results as the appears of beam at the mid span deflection whereas the basic splits
- The failure load predicted is very close to the failure load measured during experimental testing.
- Established the beam in analytical analysis carried load greater than from experiential results due to technique of presented of model in ANSYS are it ideal and it not afforded to any outside factors corresponding to the experimental results.
- The theoretical solution gives a good impression in the reinforced concrete beam strengthened by CFRP, and it is possible to dispense of experimental work.

CONCLUSIONS:

- From test results and observations, the following conclusions can be drawn:
- Using of CFRP as an external strengthening technique results in a noticeable effect on ultimate load, crack pattern, deflections and as described below:
 - Increasing the ultimate load and the capacity of the beams.
 - Delaying the crack appearance and reducing the crack width.
- The location of CFRP sheets has a major effect; attaching CFRP in bottom face in addition to side face has more effect than when attaching the same quantity of CFRP to the side faces of beams.
- In all cases in the present work, the failure in strengthened beams is caused by shear failure followed by CFRP rupture.
- The presence of external CFRP bonded to concrete beams increases the ultimate load at failure to a significant value. The maximum increase in the ultimate strength of externally strengthened beams by CFRP depends on the amount of the area and configuration of the external CFRP sheet added.

- In this study, it is observed that the use of external CFRP sheet connected to the tension sides of beams could enhance the ultimate load capacity by (58%) over the capacity of the identical unstrengthened control beam.
- Using CFRP for strengthening beams at shear zone by CFRP sheet is found successful.
- 10. The beam strengthening by shear at any compressive strength of concrete are more load capacities less than from the beam strengthening for shear and flexure.
- 11. The three-dimensional finite element model used in the present work is able to simulate the behavior of externally strengthened reinforced concrete beams by CFRP in shear and flexural groups.
- 12. The comparison between the numerical and the experimental results declared the validity of the numerical analysis and the methodology developed here where the maximum difference ratio in ultimate load was less than 13% for all the tested and analyzed beams.
- 13. The general behavior of the finite element models represented by the center span load deflection curve shows good agreement with the test results from the experimentally tested beams.

NOTATION

ACI= American Concrete Institute
ANSYS=Finite Element Computer Program
CFRP=Carbon Fiber Reinforced Polymer

REFERENCES

- ACI Committee 318, 2002, "PCA Notes on ACI 318-02 Building Code Requirement for Structural Concrete," American Concrete Institute.
- ACI Committee 318, 2008, "Building Code Requirement for Structural Concrete (ACI 318-08) and Commentary," American Concrete Institute, Farmington Hills.
- ACI Committee 440, 2002, "Guide for the design and construction of externally bonded FRP systems for strengthening of concrete structures," American Concrete Institute, Michigan, USA.

- Al-Mahaidi, R., Lee, K., and Taplin, G., "Behavior and Analysis of RC T-Beams Partially Damaged in Shear and Repaired with CFRP Laminates", Monash University, Australia; 2001, almahaidi@eng.monash.edu.au
- ANSYS, 2005, "ANSYS Help," Release 10.
- Kachlakev, D., Miller, T., "Finite Element Modeling of Reinforced Concrete Structures Strengthened With FRP Laminates", Final Report, Oregon Department of Transportation, May, 2001.

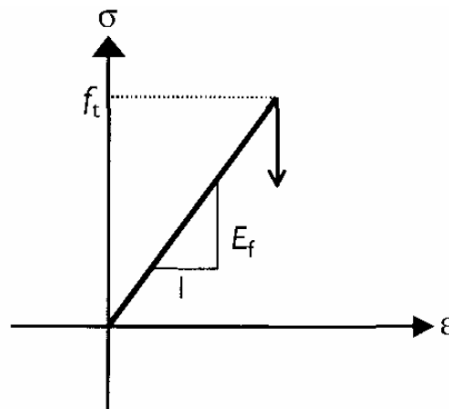


FIGURE 1, Carbon Fiber Sheet Modeling in Finite Element analysis

Table 1, Qualitative Comparison of Different Fibers Used in Composites.

Condition	Type of fibers used in composite		
	Carbon Fibers	Glass Fibers	Aramid Fibers
Tensile Strength	Very good	Very good	Very good
Young's Modulus	Very good	Good	Adequate
Long-term behavior	Very good	Good	Adequate
Fatigue behavior	Excellent	Good	Adequate
Bulk density	Good	Excellent	Adequate
Alkaline resistance	Very good	Good	Inadequate
Price	Adequate	Adequate	Very good



FIGURE 2, Carbon Fiber Sheet

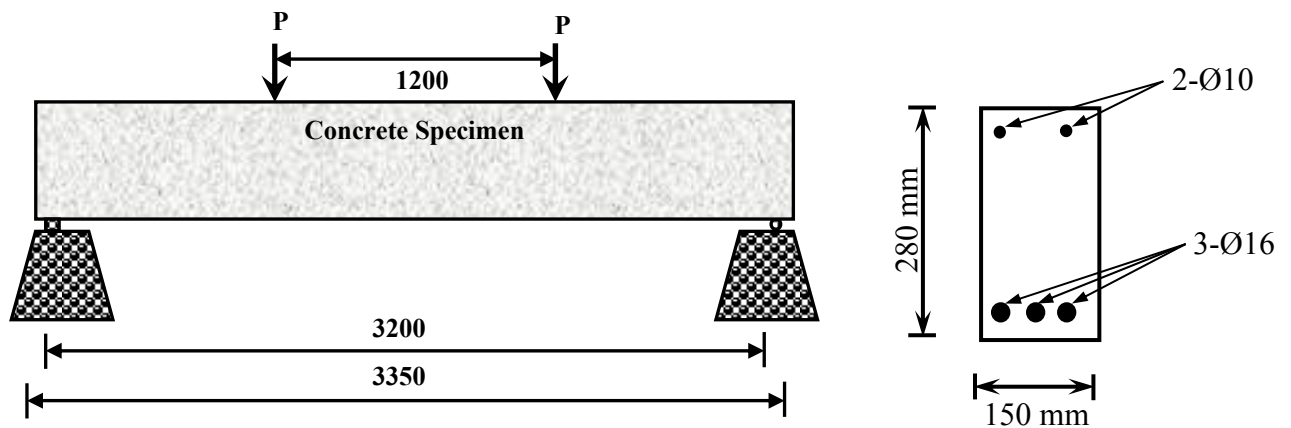


FIGURE 3, Geometry of Laboratory Specimens

Table 2, Classifications of Beams

No.	The Symbol	The Name
1	BC1	Beam Control at compressive strength equal 12 MPa
2	BS1	Beam Strengthened for shear at compressive strength equal 12 MPa
3	BF1	Beam Strengthened for shear and flexure at compressive strength equal 12 MPa
4	BC2	Beam Control at compressive strength equal 20 MPa
5	BS2	Beam Strengthened for shear at compressive strength equal 20 MPa
6	BF2	Beam Strengthened for shear and flexure at compressive strength equal 20 MPa
7	BC3	Beam Control at compressive strength equal 30 MPa
8	BS3	Beam Strengthened for shear at compressive strength equal 30 MPa
9	BF3	Beam Strengthened for shear and flexure at compressive strength equal 30 MPa
10	BC4	Beam Control at compressive strength equal 39 MPa
11	BS4	Beam Strengthened for shear at compressive strength equal 39 MPa
12	BF4	Beam Strengthened for shear and flexure at compressive strength equal 39 MPa

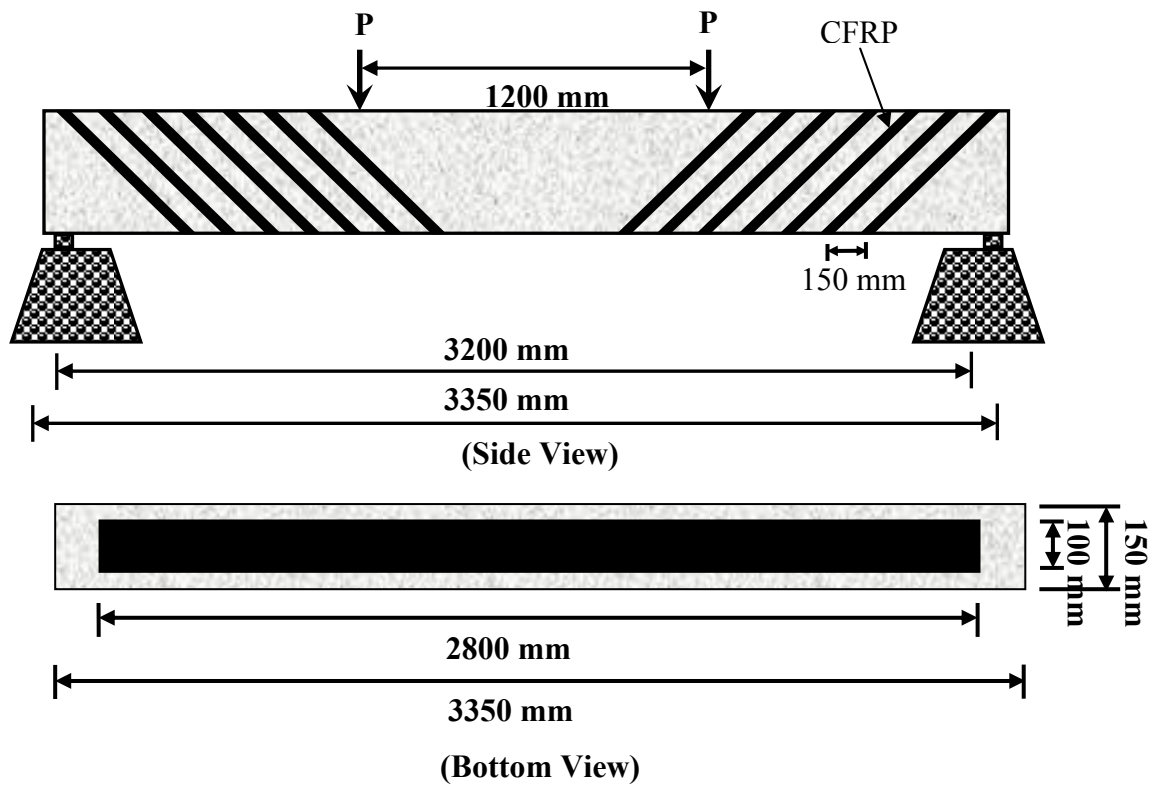


FIGURE 4, Specimens with CFRP in Flexure Zone



FIGURE 5, Demec Points in Concrete and CFRP

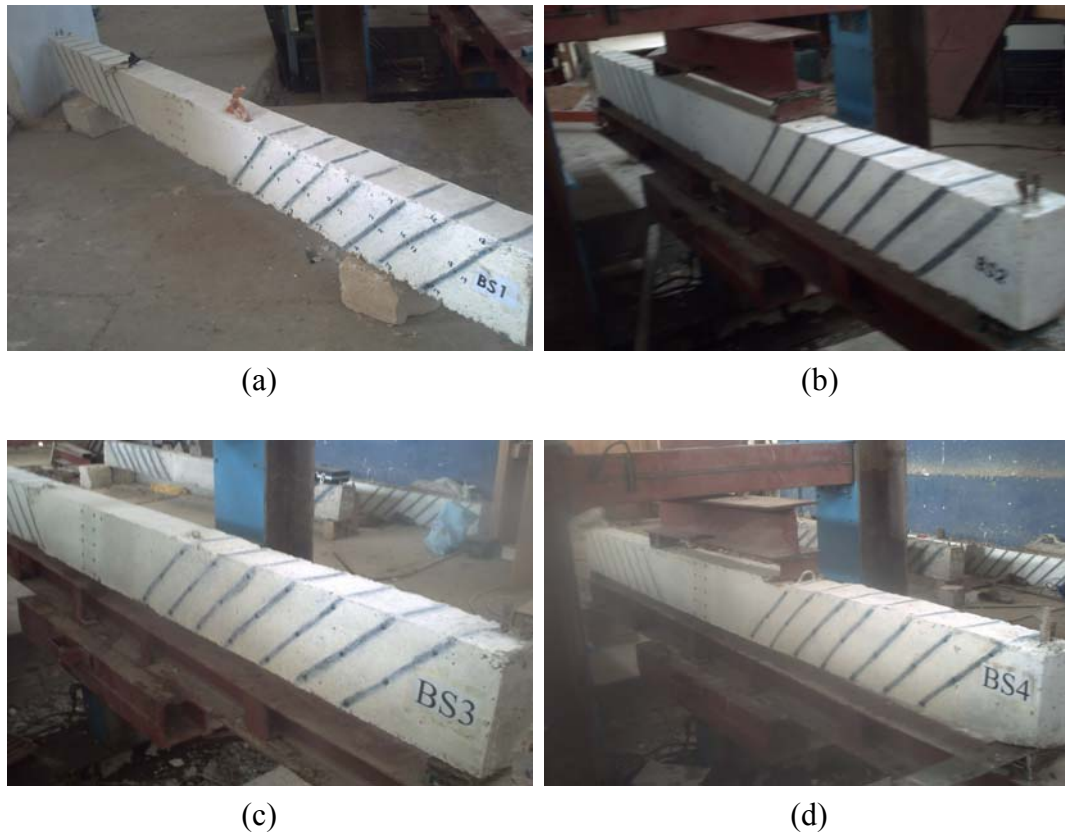


FIGURE 6, Beams Strengthened for Shear ($f'_c=12, 20, 30$ and 39 MPa)

Table 4, Experimental results of the tested beams.

Group no	Beam designation	crushing strengths (MPa)	Total applied load (KN)	Mid-span deflection (mm)	Percentage increase in ultimate load with respect to reference beam %	Percentage increase in ultimate deflection with respect to reference beam %
			P_u	u		
1	BC1	12	45	9.229	-----	-----
	BS1	12	65	22.625	44.4	145.2
	BF1	12	70	29.445	55.5	219
2	BC2	20	58	13.348	-----	-----
	BS2	20	69	21.679	19	62.4
	BF2	20	80	27.81	37.9	108.3
3	BC3	30	60	14.498	-----	-----
	BS3	30	71	19.702	18.3	35.9
	BF3	30	95	31.236	58.3	115.5
4	BC4	39	80	15.41	-----	-----
	BS4	39	95	23.318	18.8	51.33
	BF4	39	104	32.1	30	108.3

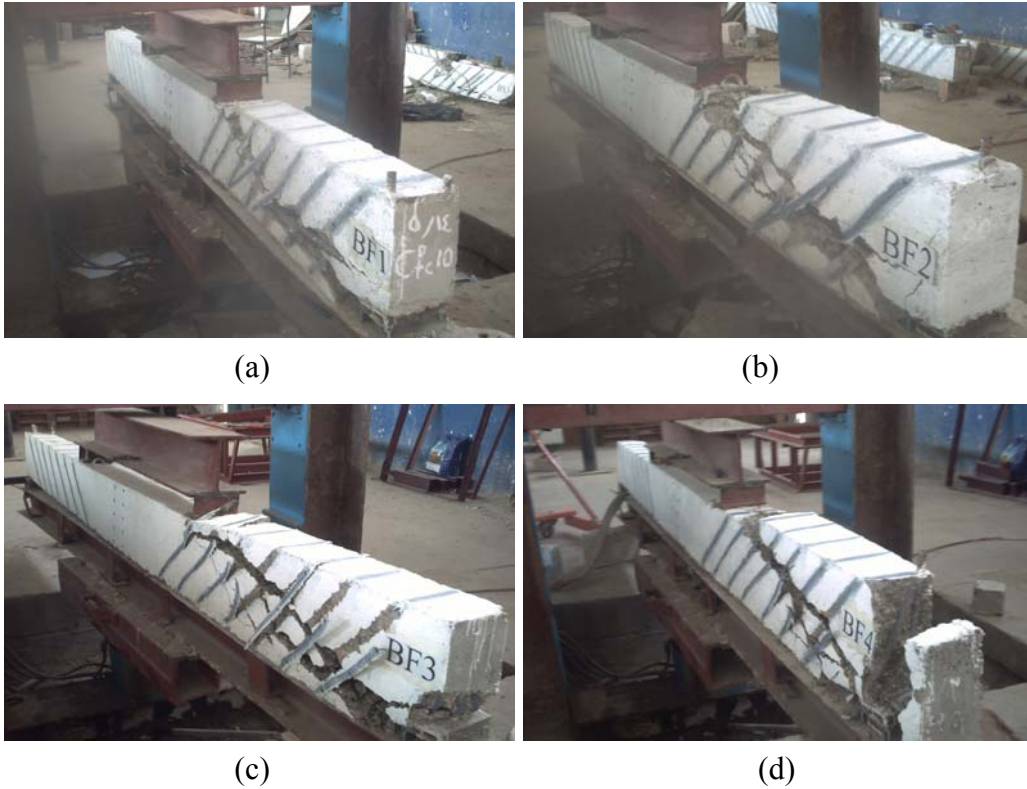
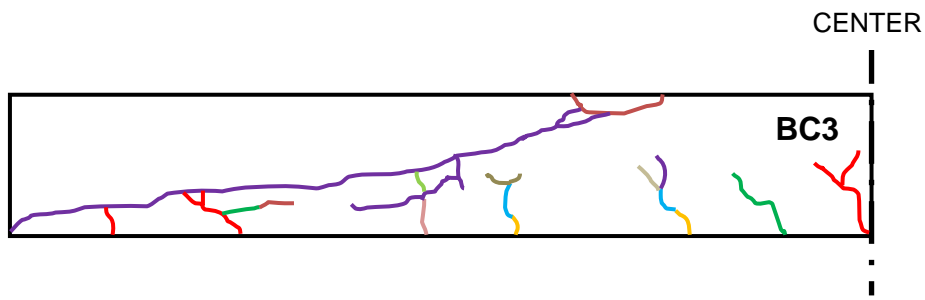
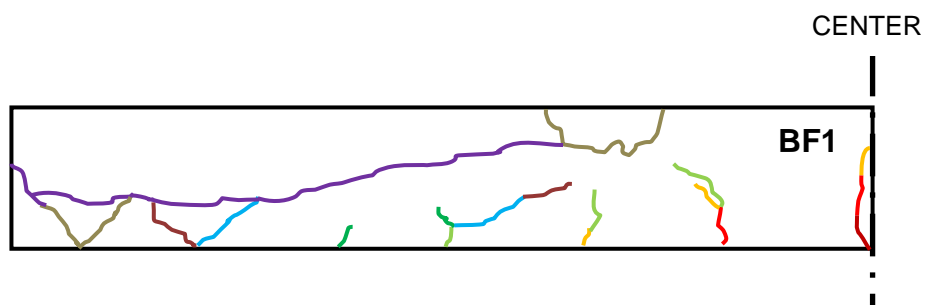


FIGURE 13, BF1, BF2, BF3 and BF4 After Tested



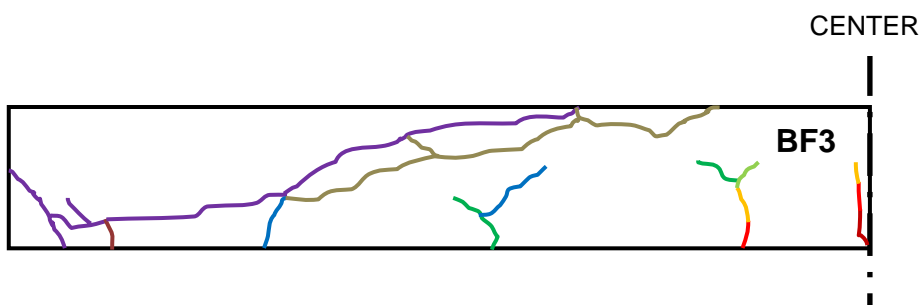
color	Load (kN)
	10
	20
	25
	35
	40
	45
	50
	55

(a)



color	Load (kN)
	15
	20
	30
	40
	50
	60
	70
	73

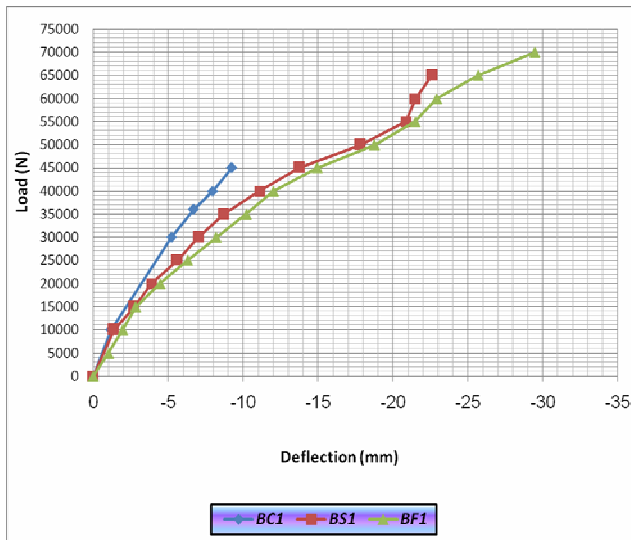
(b)



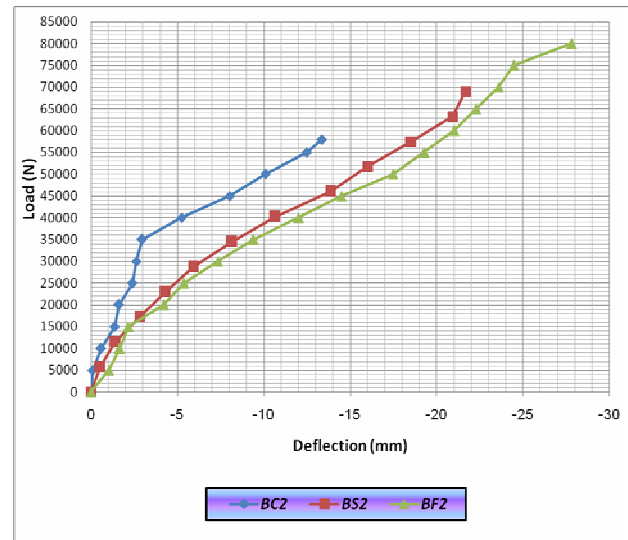
color	Load (kN)
	20
	30
	40
	50
	60
	70
	80
	85
	95

(c)

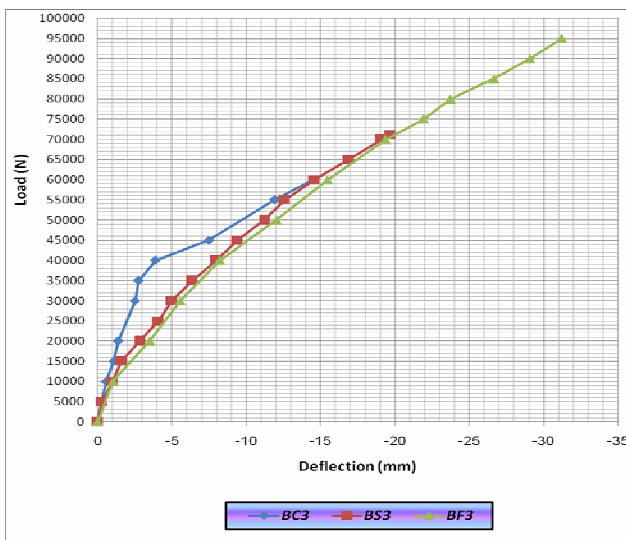
FIGURE 8, Crack Patterns for BC3, BS3 and BF3 respectively



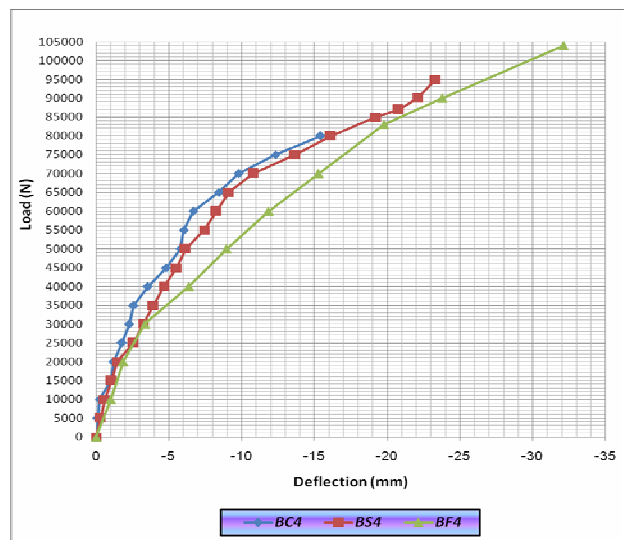
(a)



(b)



(c)



(d)

FIGURE 9, Load-Deflection Curves for Beams having between Beams at $f'_c=12, 20, 30$ and 39 MPa respectively

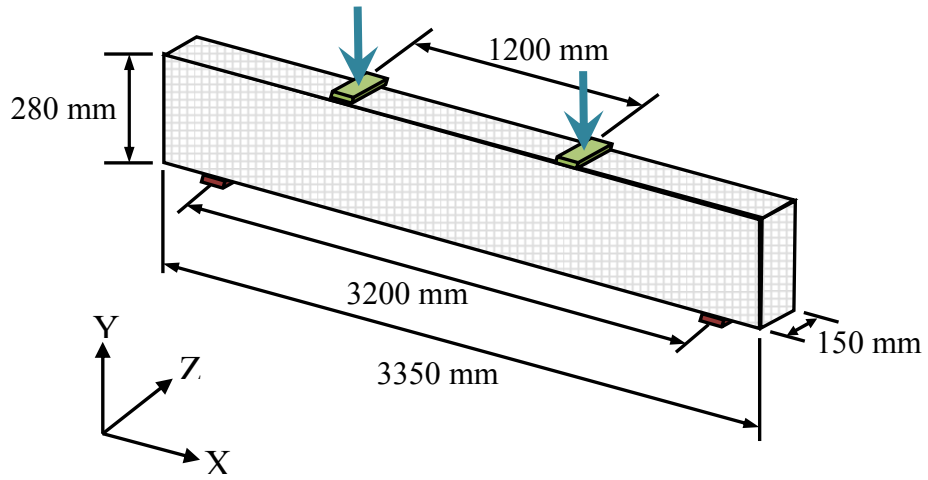


FIGURE 10, Typical Beam Dimensions (Not to Scale)

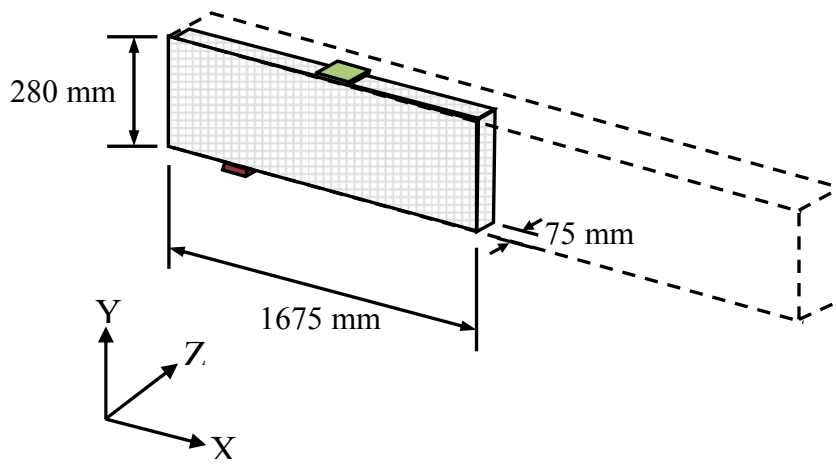


FIGURE 11, Use of A Quarter Beam Model (Not to Scale)

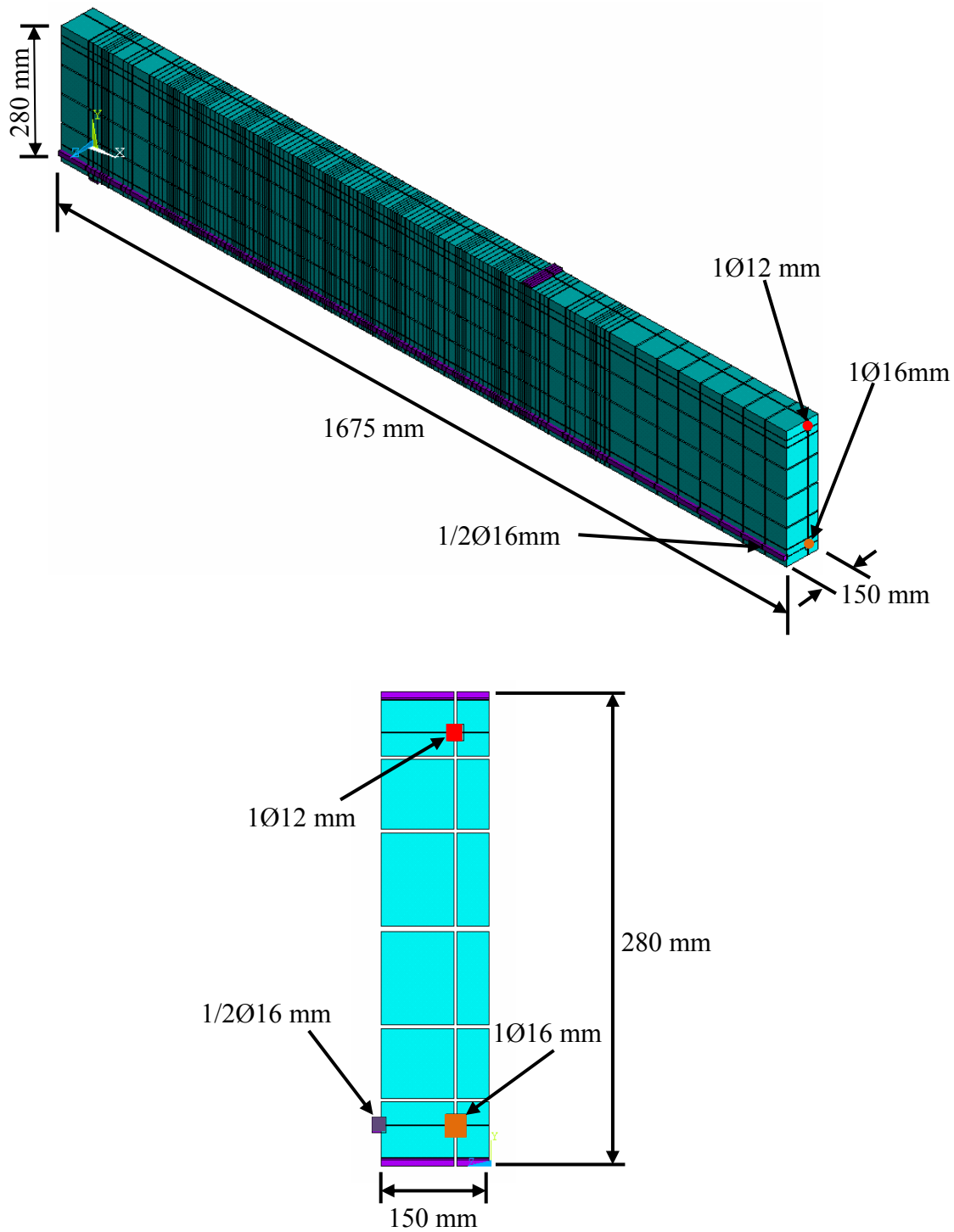
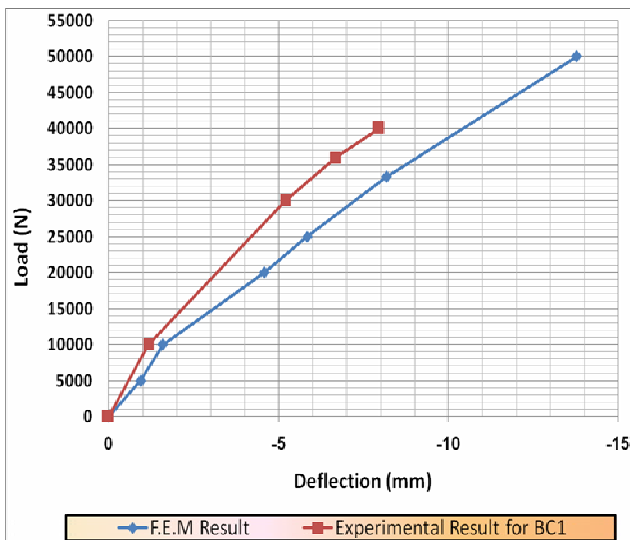


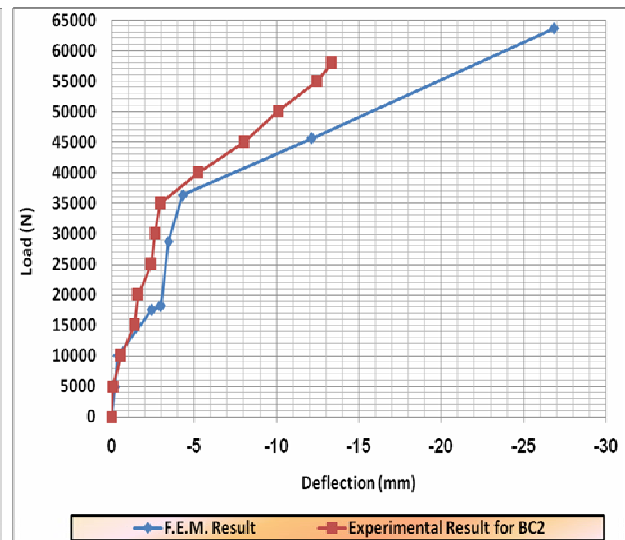
FIGURE 12, Typical Steel Reinforcement for A Quarter Beam Model (Not to Scale)

Table 5, Comparisons between experimental and numerical ultimate loads

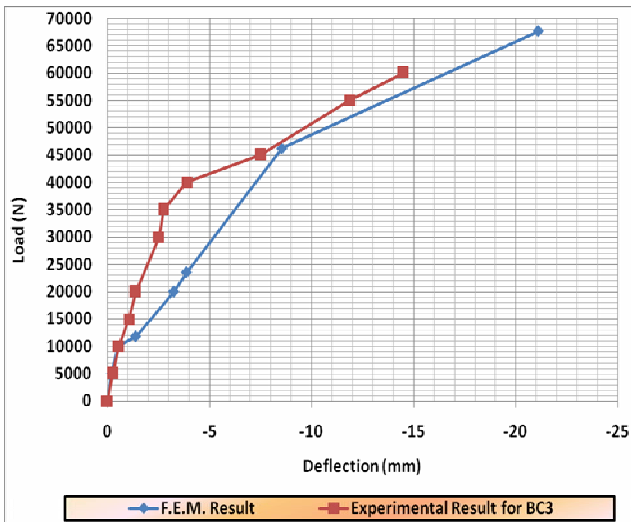
Beam designation	Numerical ultimate load (kN)	Experimental ultimate load (kN)	P_{num}/P_{exp}
<i>BC1</i>	50.0	45	1.11
<i>BS1</i>	70.0	65.0	1.08
<i>BF1</i>	74.7	70.0	1.07
<i>BC2</i>	63.6	58.0	1.09
<i>BS2</i>	66.7	69.0	0.97
<i>BF2</i>	80.0	80.0	1.00
<i>BC3</i>	67.6	60.0	1.13
<i>BS3</i>	77.8	71.0	1.10
<i>BF3</i>	90.0	95.0	0.95
<i>BC4</i>	88.5	80.0	1.11
<i>BS4</i>	100.0	95.0	1.05
<i>BF4</i>	106.0	104.0	1.02



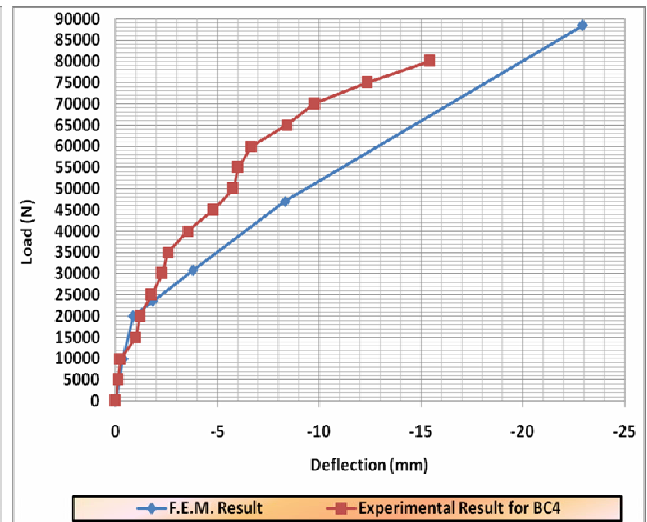
(a)



(d)

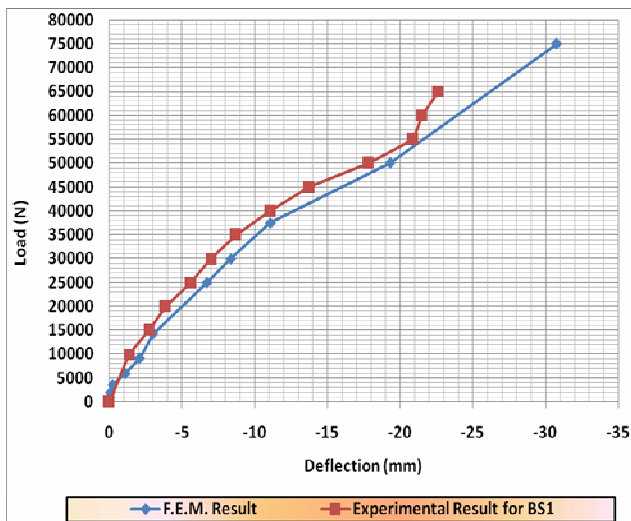


(c)

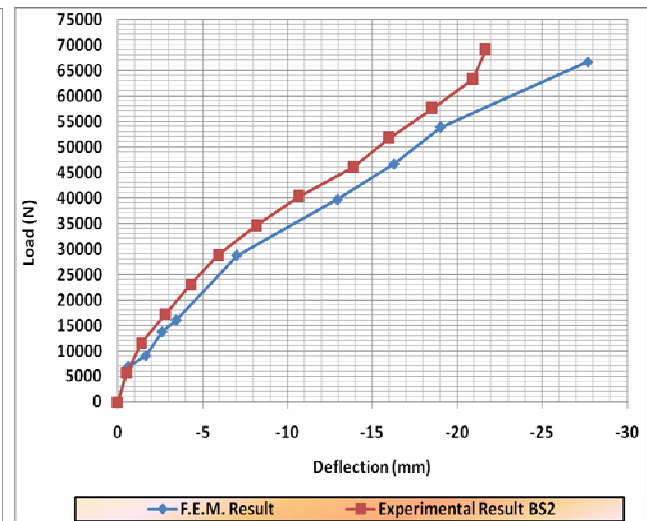


(d)

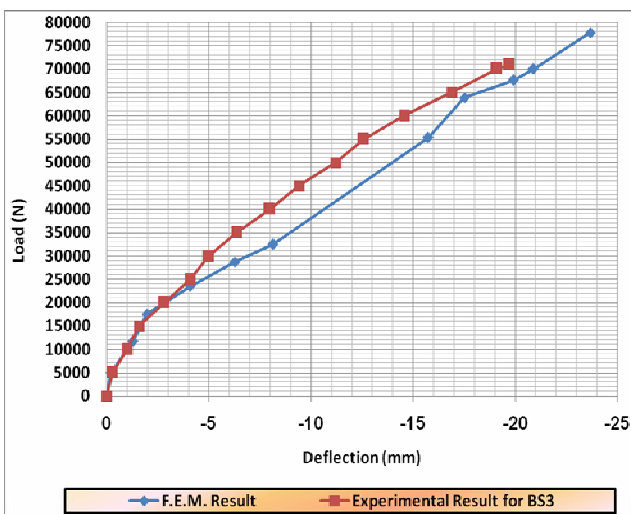
FIGURE 31, Load-Deflection Curve BC1, BC2, BC3 and BC4 respectively



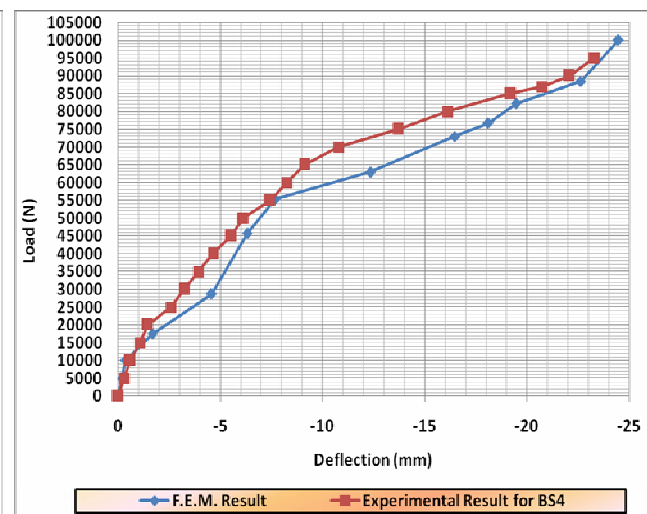
(a)



(b)

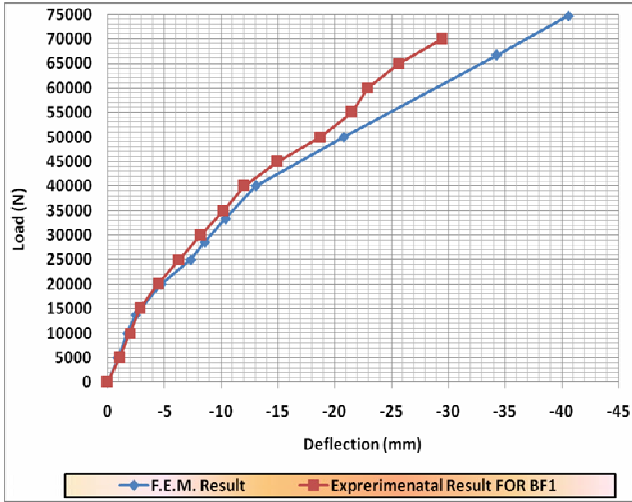


(c)

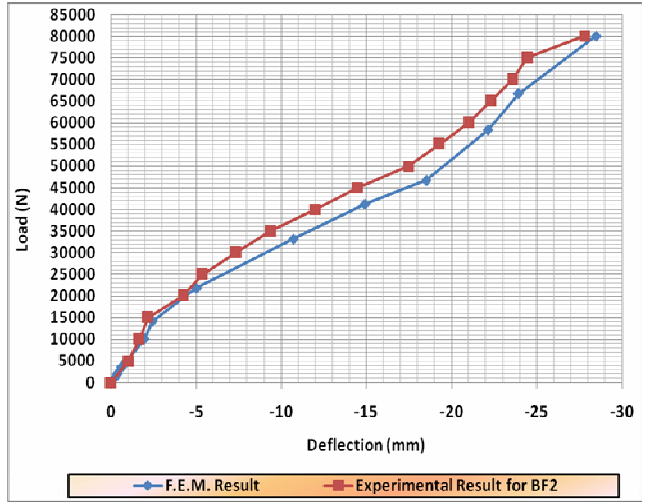


(d)

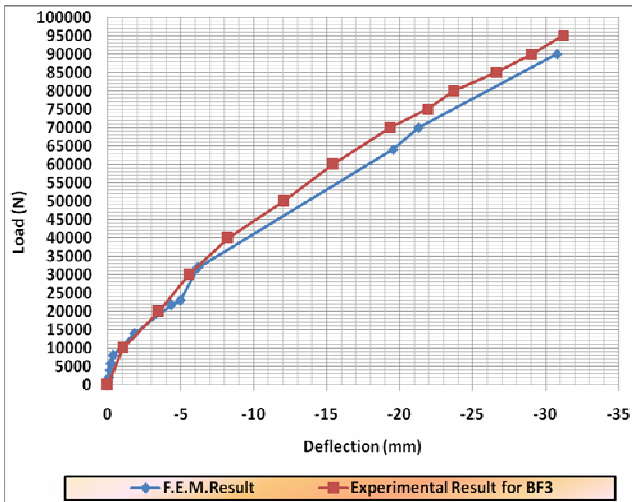
FIGURE 32, Load-Deflection Curve BS1, BS2, BS3 and BS4 respectively



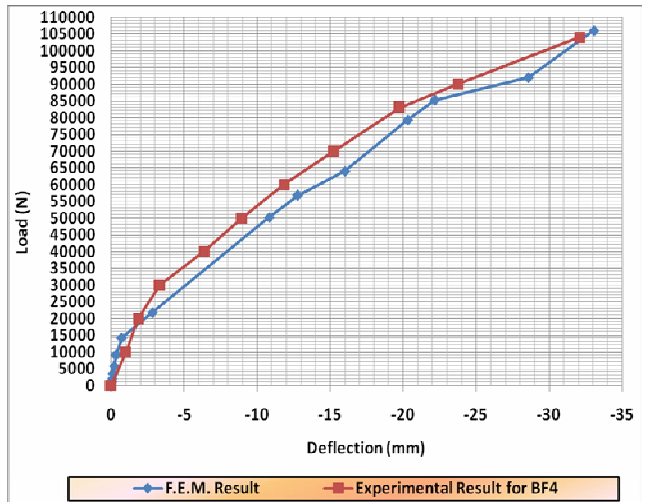
(a)



(b)



(c)



(d)

FIGURE 33, Load-Deflection Curve BF1, BF2, BF3 and BF4 respectively